Effect of T-T Base Mismatches on Three-Arm DNA Junctions†

Min Zhong, Michael S. Rashes, and Neville R. Kallenbach*

Department of Chemistry, New York University, New York, New York 10003

Received January 6, 1993; Revised Manuscript Received April 13, 1993

ABSTRACT: In contrast to four-arm immobile DNA junctions, three-arm DNA junctions have unique structural and dynamic properties consistent with lack of a single dominant conformation. The effect of T-T base mismatches at the branch in a three-arm model junction has been investigated using a combination of electrophoretic mobility measurements, chemical footprinting experiments, and thermodynamic studies. The results indicate that three-arm junctions are only slightly destabilized by a mismatch flanking the branch, relative to four-arm junctions. The effect of a mismatch varies with the sequence and position of the site of the mismatch. Since a three-arm junction with two mismatches flanking the branch is as stable as two junctions each with a single mismatch, the stability of three-arm junctions is not determined by stacking interactions at the branch in a simple way. The properties of three-arm junctions with one or two mismatches are consistent with a picture in which the conformation is the result of several substrates in which base pairs flanking the branch are transiently open, allowing bases to interact with the remaining duplexes.

The folded structure of cellular RNA molecules includes branches with three helical arms (Gluick & Draper, 1992). The interactions responsible for stabilizing these structures are of interest. This form of branched structure arises less frequently in duplex DNA, although palindromic sequences capable of forming branches in single strands are not infrequent in nature, and these will contribute intermediate states (*via* hairpin formation) during any process that favors single strands, such as replication or thermal unfolding of a duplex. The geometry and stabilization of three-arm junctions in DNA are thus of interest in terms of understanding intermediates that arise during unfolding, recombination, or repair of DNA. In particular, developing a quantitative model for the thermal unfolding of any sequence of DNA is an exercise of concern in the design of PCR assays, for example (Saiki et al., 1988). At present, the thermodynamic parameters determined from short DNA duplexes (Breslauer et al., 1986) fail to account for those of longer molecules (Gotoh & Tagashira, 1981). Even short DNA dumbbells reveal parameters inconsistent with those from very short duplexes (Doktycz et al., 1992). One obvious factor that has not been taken into account is the contribution of branched states in the population of intermediates that arise as the strands of the duplex unwind. A complete treatment of the unfolding of DNA at any salt concentration [see Goldstein and Benight (1992)] thus requires that branched states be accounted for thermodynamically, including mismatches of different kinds; the experiments reported here lay a foundation for this description. In addition, geometrical and ligand binding properties of three-arm branched states are described, which again will prove useful in trying to understand the conformational properties of partially unfolded duplexes and how these interact with ligands. Finally, in trying to derive rules for predicting the conformation and stability of structure in RNA, the behavior of the corresponding sequences in DNA provides a useful benchmark. Evidence is accumulating, for example, that several regions in RNA that were thought to be unpaired are not (Draper, 1992). The absence or presence of such structure in deoxy sequences tells us something about the interactions responsible.

Three-arm structures (Minagawa et al., 1983) have been reported to accumulate in DNA isolated from T4 bacteriophage mutants deficient in the gene 49 product endonuclease VII (Mizuuchi et al., 1982). The enzyme indiscriminately cleaves three- and four-arm junctions in vitro, and may function in several DNA-processing steps besides recombination (Broker & Doermann, 1975). Several lines of evidence suggest that the branch in three-arm DNA junctions behaves as a relatively open structure compared to duplex DNA or immobile four-arm junction models [reviewed by Lu et al. (1992)], as well as branched RNAs. The three-arm branches that accumulate in gene 49 phage T4 mutants are highly susceptible to single-strand-specific nucleases (Minagawa et al., 1983), possibly because of the presence of single-strand regions. Synthetic models for three-arm DNA junctions are susceptible to single-strand-specific reagents at the branch (Duckett & Lilley, 1990; Guo et al., 1990), indicating this is a property of the branch itself. Three-arm DNA junctions possess an asymmetric structure in the presence of Mg^{2+} or other cations (Guo et al., 1990; Lu et al., 1991), but with very different properties from those of immobile four-arm junctions. Bases at the branch in four-arm junctions are resistant to cleavage by single-strand-specific chemical probes [see Lu et al. (1992)] as well as to single-strand-specific endonucleases. Sticky-ended versions of three-arm junctions cyclize upon ligation to yield circular products that include trimers and tetramers as well as longer chains, implying that there is considerable flexibility at the branch (Ma et al., 1986). Similarly, Jensch and Kemper (1986) have noted that a restriction site spanning the branch in a three-arm junction is susceptible to the enzyme on each arm of the junction. The structure of the three-arm junction models is by no means symmetric, lacking helix–helix interactions among the arms at the branch [see Duckett and Lilley (1990)]. Analysis of the conformation by mobility experiments indicates an asymmetric structure, as does the pattern of reactivity of sites in three-arm junctions to single-strand-specific chemical probes (Guo et al., 1990).

In a series of experiments on three-arm junctions containing extra bases at the branch, Leontis's group (1991) has reported

† This research was supported by Grant CA24101 from the National Cancer Institute, NIH.

* Author to whom correspondence should be addressed.

0006-2960/93/0432-6898$04.00/0

the interesting result that inserting two A's stabilizes the junction. This latter observation suggests that conformational strain might exist in three-arm junctions that can be reduced by inserting added bases. Another way to relax the structure conformationally is to introduce mismatches at the branch. This possibility has prompted us to investigate the effect of base mismatching at the branch on the stability of three-arm DNA junctions. The mismatch we have chosen for analysis, T-T, is one in which pairing and stacking are both weak (Aboul-Ela et al., 1985), making it likely to provide a source of conformational freedom. We have previously reported that T-T mismatches flanking the branch specifically destabilize the structure of four-arm immobile DNA junctions in the presence of Mg^{2+} (Zhong et al., 1992), but with effects that are not seen in T-T mismatches in a duplex. A more extensive survey by Duckett and Lilley (1991) suggests that this is a general property of mismatches in four-arm junctions, which have a defined structure in the presence of Mg^{2+} (Cooper & Hagerman, 1987; Duckett et al., 1988). The question we ask here is how the stability and geometry of three-arm junctions respond to base mismatching at the branch, and in particular whether aspects of the underlying conformational dynamics in three-arm junctions are revealed in these experiments.

MATERIALS AND METHODS

Synthesis and Purification of Oligonucleotides. Oligonucleotides used in this study were synthesized on an Applied Biosystems 391 automated DNA synthesizer, deprotected by routine phosphoramidite procedures (Caruthers, 1982), and purified by ion-exchange HPLC (Du Pont Zorbax Bio Series oligonucleotide column) or polyacrylamide gel electrophoresis. 5′-Terminal labeling used bacteriophage T4 polynucleotide kinase (Bethesda Research Laboratories) and [γ-^{32}P]ATP; the labeled strands were purified by polyacrylamide gel electrophoresis. The concentration of strands in stock solutions was determined spectrophotometrically at 260 nm and 80 °C, using the nearest-neighbor values of Cantor *et al.* (1970).

Annealing Reactions. These were carried out by mixing stoichiometric concentrations of the appropriate DNA strands in 50 mM Tris·HCl (pH 7.5) with 10 mM $MgCl_2$, heating at 90 °C for 2 min, cooling slowly to room temperature, and finally chilling to 4 °C.

Gel Electrophoresis. Unless otherwise indicated, the native gels contained 18% polyacrylamide (19:1 monomer:bis ratio), and the running buffer contained 40 mM Tris, 20 mM acetic acid, and 2 mM $MgCl_2$ (pH 8.1). Gels were run at 8 V/cm, cooled by a circulating water bath (4 °C), and stained in 11:9 formamide/water containing 0.01% Stains-All dye or exposed for 1 h without an intensifying screen. For denaturing gels, the products of cleavage reactions were taken up in formamide-loading buffer, heated to 90 °C for 1 min, chilled to 0 °C, and run on 20% polyacrylamide (19:1 monomer:bis ratio)/7 M urea gels for 2.5 h at 2000-V constant voltage (ca. 50 V/cm) and 40 °C. Gels were dried immediately on a vacuum drying apparatus (Hoefer) and exposed to X-film at −70 °C using a Du Pont Cronex Lightning Plus intensifying screen.

Elongation of DNA Molecules. The 60 bp DNA reporter fragment with natural sequence used in this study is formed by mixing stoichiometric concentrations of a synthetic 58-nucleotide strand with a complementary 5′-phosphorylated 62-nucleotide strand. The reporter duplex thus contains a blunt end with a four-base, 5′ overhang that is *Eco*RI-derived. Elongation of branched DNAs containing a pseudo-*Eco*RI end is achieved by ligation to the synthetic reporter fragment,

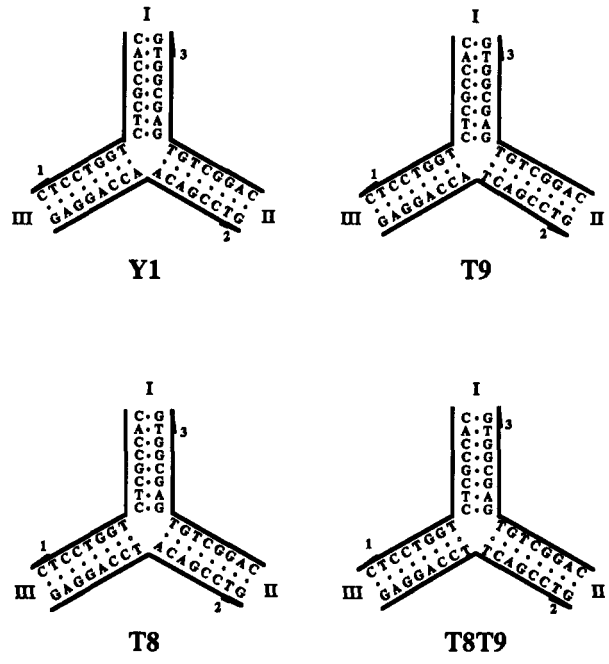

FIGURE 1: Sequences and schematic representations of the four synthetic DNA three-arm junctions used in this study. Each molecule consists of three 16-mer strands of DNA. The 3′ ends of the strands are indicated by half-arrowheads. The strand numbering indicated in this figure is used throughout the text.

as described by Copper and Hagerman (1987, 1989). Ligation reactions with T4 DNA ligase (Bethesda Research Laboratories) were carried out in 50 mM Tris·HCl (pH 7.5), 10 mM $MgCl_2$, 1 mM ATP, and 1 mM dithiothreitol at 16 °C overnight. Following heat inactivation (65 °C for 5 min), ligase was removed by phenol extraction, and DNA was precipitated by ethanol.

Elongated branched DNA halves or extended branched DNAs were purified on 6% polyacrylamide gels.

UV Melting Curves. Absorbance versus temperature profiles (melting curves) for the DNA molecules, at various strand concentrations in a 20 mM sodium cacodylate buffer containing 100 mM NaCl and 1 mM $MgCl_2$ (pH 7.0), were recorded at 260 nm on a thermoelectrically controlled Perkin-Elmer 552 spectrophotometer interfaced to a PC-XT computer for acquisition and analysis of experimental data. The temperature was scanned at a heating rate of 1 °C/min. These melting curves allow us to measure the transition temperatures, T_m, the midpoints of the order–disorder transition of these DNA molecules, and to determine the associated van't Hoff thermodynamic parameters (Marky & Breslauer, 1987), by applying a two-state approximation to the helix–coil transition of each molecule. The validity of this approximation for a branched molecule such as J1 has been discussed by Marky et al. (1987).

Differential Scanning Calorimetry. The total heat of the helix–coil transition of each DNA molecule was measured directly with a Microcal MC-2 differential scanning calorimeter (DSC) interfaced to an IBM PC computer. A typical solution for these experiments contained 20 mM sodium cacodylate, 100 mM NaCl, and 1 mM $MgCl_2$ (pH 7.0) with a total strand concentration of 0.2–0.3 mM and was scanned from 0 to 95 °C at a heating rate of 45 °C/h. A buffer alone was used as blank; a buffer vs buffer scan was subtracted from the sample scan and normalized for the heating rate. The area of the resulting curve is proportional to the transition heat; normalized for the number of moles, this heat gives the

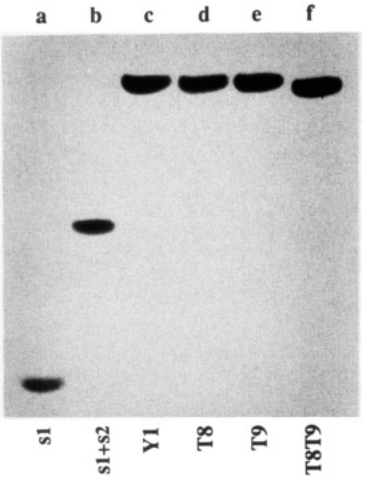

FIGURE 2: Polyacrylamide gel electrophoresis of oligodeoxynucleotide strands and mixtures. A photograph of a native gel is shown in which the junction components have been combined in equimolar combinations to illustrate their association under conditions of electrophoresis. Each lane contains 3.0 μg of each strand alone or in combination with others. The numbering convention refers to that of Figure 1. Note that the trimeric junction migrates as a single well-defined band with lower mobility than either monomer or dimer.

transition enthalpy ($\Delta H°_{cal}$). The DSC curves also allow one to estimate the transition entropy ($\Delta S°$) and free energy ($\Delta G°$) from the area of $\Delta C_p/T$ vs T with the Gibbs equation, respectively.

Chemical and Enzymatic Cleavage Reactions. (*a*) *Cleavage by Neurospora crassa Endonuclease.* An ammonium sulfate suspension of endonuclease from *Neurospora crassa* (Boehringer Mannheim) was centrifuged and the precipitated enzyme dissolved in 50 mM Tris·HCl (pH 8.0) with 10 mM $MgCl_2$. The exonuclease activity with double-stranded DNA was removed by preincubation at 37 °C for 1 h (Fraser, 1980). Digestions of DNA molecules (10 μM) with 1 μg of endonuclease were performed in 10 μL of 50 mM Tris·HCl (pH 8.0) with 10 mM $MgCl_2$ for 5 min at 4 °C. Reactions were stopped by rapid ethanol precipitation and lyophilized.

(*b*) *Cleavage by DNase I.* A stock solution of DNase I (Sigma, bovine pancreatic) was prepared by dissolving the dry enzyme in 50% glycerol/50 mM Tris·HCl (pH 7.0) and stored at −20 °C. This solution was diluted with DNase I buffer (50 mM Tris·HCl, pH 7.0, 32 mM $MgCl_2$, and 8 mM $CaCl_2$) to provide activated enzyme. For cleaving DNA molecules, 10-μL DNA samples (10 μM) were exposed to 0.2 unit of the activated DNase I complex for 5 min at 4 °C. Reactions were stopped by rapid ethanol precipitation and lyophilized.

(*c*) *Osmium Tetroxide Modification.* DNA samples (10 μM) were incubated with 1 mM osmium tetroxide (OsO_4) and 3% pyridine in 50 mM Tris·HCl (pH 7.5) with 10 mM $MgCl_2$ at 4 °C for 10 min (Lilley & Palecek, 1984). Reactions were stopped by two sequential ethanol precipitations, and the mixes were lyophilized. The DNAs were cleaved at the site of reaction by treatment with 100 μL of 1 M piperidine at 90 °C for 30 min and lyophilized.

(*d*) *Diethyl Pyrocarbonate Modification.* Branched DNAs were modified by diethyl pyrocarbonate (DEPC) essentially as described by Herr (1985). DNAs (10 μM) were suspended in 10 μL of 50 mM Tris-HCl (pH 7.5) with 10 mM $MgCl_2$ and incubated with 1 μL of DEPC for 60 min at 4 °C. The reactions were terminated by two sequential rapid ethanol precipitations and then lyophilized. The DNAs were cleaved

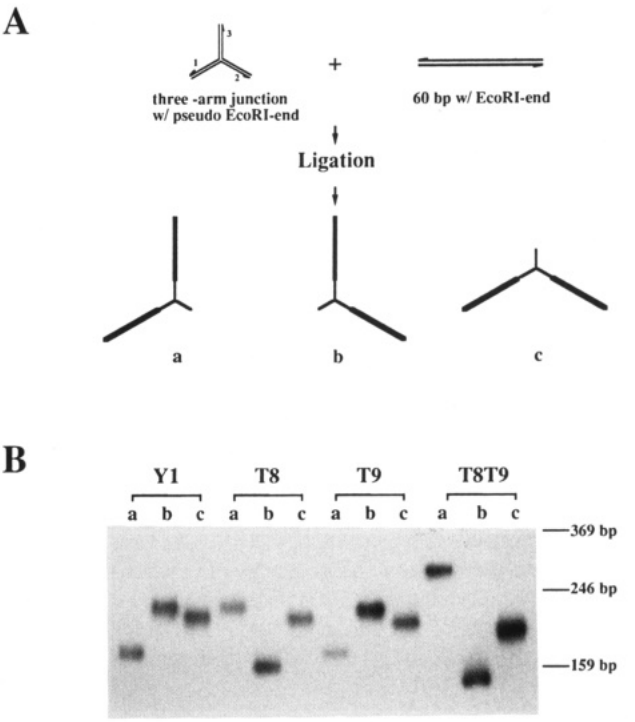

FIGURE 3: (A) Outline of construction of three possible species for analysis by polyacrylamide gel electrophoresis. A radioactively labeled DNA junction with two pseudo-*Eco*RI ends is ligated to the *Eco*RI-ended reporter fragment (Cooper & Hagerman, 1987). (B) Gel electrophoretic analysis of DNA junctions with two arms extended. The ordering of these samples is the same as in Figure 3A. The radioactive DNA samples were electrophoresed in a 12% polyacrylamide gel, followed by autoradiography. Note that in T8 and T8T9 the mobility pattern of the three species is very deferent from those of Y1 and T9, consistent with geometric changes at the branch.

at the sites of DEPC modification by treatment with 100 μL of 1 M piperidine at 90 °C for 30 min and lyophilized.

(*e*) *Cleavage by MPE·Fe(II).* DNA samples (10 μM) were exposed to 10 μM (Fe(II) and 10 μM MPE (van Dyke & Dervan, 1983) in a buffer containing 10 mM Tris·HCl (pH 7.5) with 50 mM NaCl and 10 mM $MgCl_2$ for 15 min at 4 °C, followed by addition of 4 mM dithiothreitol for 60 min, and the reaction was stopped by rapid ethanol precipitation and lyophilized.

For porphyrin binding experiments, DNA samples were incubated with a 10 μM sample of the free base tetrapyridylporphyrin, H_2TMpyP-4 (Mid-Century Chemical Co.), and 10 μM MPE·Fe(II) in a buffer containing 10 mM Tris·HCl (pH 7.5) with 50 mM NaCl and 10 mM $MgCl_2$ for 15 min at 4 °C, followed by addition of 4 mM dithiothreitol for 60 min, and the reaction was stopped by rapid ethanol precipitatin and lyophilized.

Sequencing Reaction. Purine-specific (A+G) sequencing ladders were generated from each 5′ ^{32}P-labeled oligonucleotide using the piperidine–formate reaction (Maxam & Gilbert, 1980).

Densitometry. Autoradiograms were scanned on a Hoefer GS300 densitometer, without base-line corrections.

RESULTS

Formation of Three-Arm Junctions Containing T-T Mismatches. To establish that the strands containing mismatched bases assemble in the anticipated manner to form three-arm junctions, we carried out native gel electrophoresis on mixtures

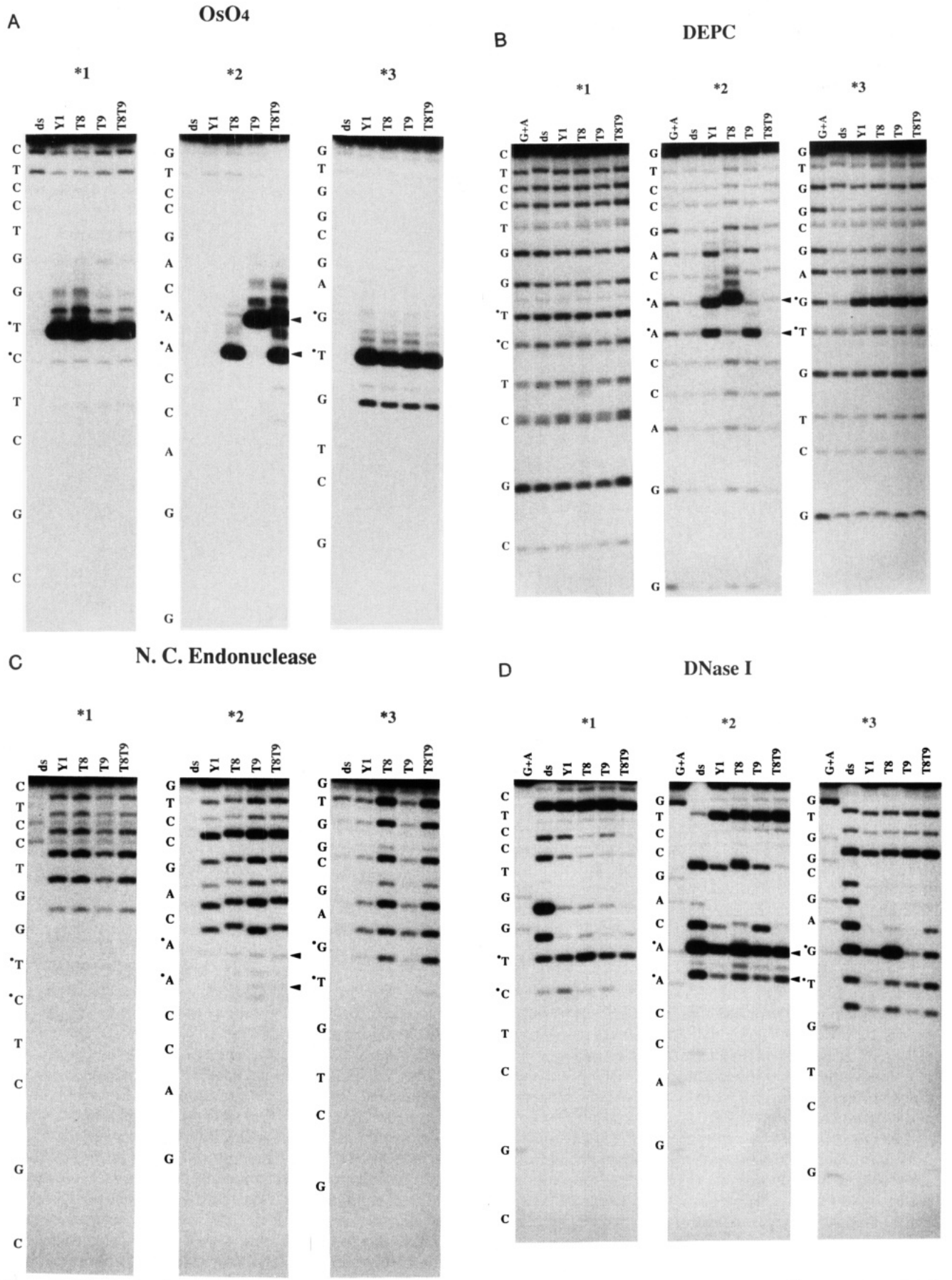

FIGURE 4: **Chemical and enzymatic reactions. Autoradiographs** of the gels are shown. Junctions 5′-labeled with ^{32}P were cleaved with OsO_4/piperidine (A), DEPC/piperidine (B), *Neurospora crassa* endonuclease (C), and DNase I (D) and electrophoresed on a sequencing gel alongside A + G sequence markers derived from the same radioactive strand. The reactions were carried out as described under Materials and Methods. Radioactively labeled strands are indicated by the number of the strand in the 5′ half. Arrows indicate the sites of thymine substitution in mismatched junctions.

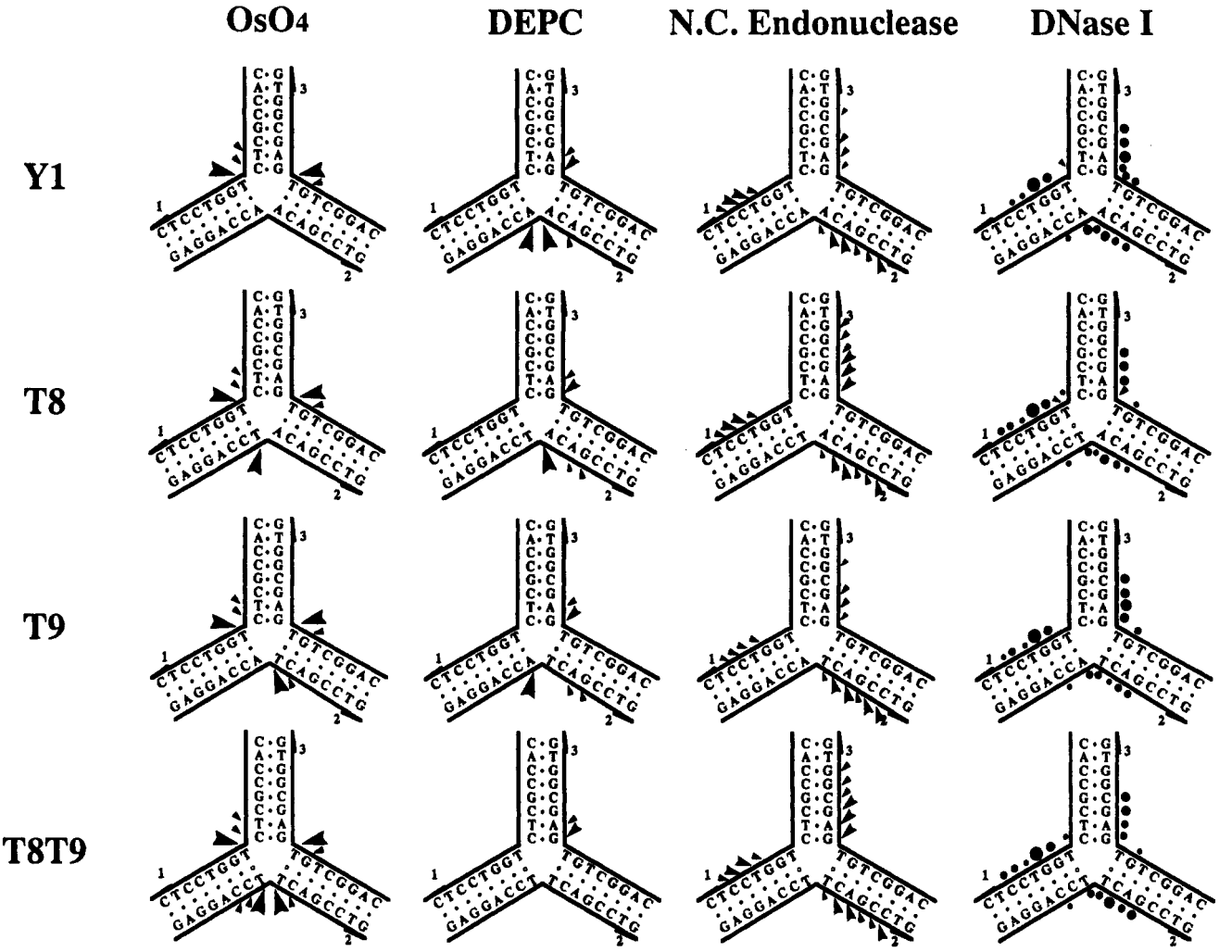

FIGURE 5: Sites of differential enhancement and protection in Y1, T8, T9, and T8T9 are compared to those in the duplex. Arrows represent enhancement whereas filled circles indicate protection. The size of the arrow and the circle is a measure of the quantitative intensity of each responsive site.

of pairs and triples of the strands illustrated in Figure 1. Lanes a, b, and c in Figure 2 indicate respectively the mobility of strand 1 alone, an equimolar mixture of strands 1 + 2, and an equimolar mixture of strands 1 + 2 + 3, forming the control junction Y1, which lacks any mismatched pairs. The numbering of these strands is as shown in Figure 1. The three-arm complex has a unique mobility that is much slower than that of any combination of pairs of the arms (Ma et al., 1986; Guo et al., 1990). The three strands containing T-T mismatches flanking the branch similarly form trimeric complexes, with mobilities that differ only slightly from that of Y1 (lanes d–f). No trailing of bands indicative of dissociation of the complexes is seen in this experiment, implying that each of the complexes sketched in Figure 1 is stable at low temperature in the presence of Mg^{2+}.

Analysis of the Mobilities of Four Three-Arm Junctions Containing Pairs of Extended Arms. Cooper and Hagerman (1987) have introduced an experimental procedure for evaluating the geometric properties of branched DNA molecules. Applied to the case of a three-arm junction, long duplex DNA reporter arms are ligated pairwise to the ends of a junction, forming a set of three structures with reporter arms as shown in Figure 3. The mobility of the resulting set of structures is measured in native PAGE. If the geometry of a junction is asymmetric, one or another of these structures is expected to show a migration anomaly relative to the others. This expectation is based on the analogous behavior of DNA molecules in which the helix axis bends, an effect that reduces the mobility of a structure containing extended duplexes on either side of the bending sequence (Koo et al., 1986). The method has been used to define the preferred stacked conformation of four-arm junctions in the presence of Mg^{2+} (Cooper & Hagerman, 1987, 1989; Duckett et al., 1988). Figure 3A summarizes the constructions used in our present experiments. For each of the four junctions studied, 60 bp reporter arms are appended pairwise to the three arms, giving the three species designated as **a**, **b**, and **c** in the figure. In **a**, the twelve o'clock and eight o'clock arms are extended by this length, for example, whereas in **c**, the four o'clock and eight o'clock arms are extended. If the angles in the **a**, **b**, and **c** extended complexes were as sketched in Figure 3A, or if the branches in the three-arm structures were perfectly flexible, we would anticipate that each of the complexes **a**, **b**, and **c** would have the same mobility. As seen in Figure 3B, this result is not observed for any of the junctions with the sequences shown in Figure 1. Three-arm junctions are thus neither symmetric nor fully flexible, even at low temperature. According to the reference mobilities indicated to the left of the bands in Figure 3B, junctions Y1 and T9 have very similar patterns in the mobility of the extended complexes. In each case, **a** travels with a mobility close to that of a fully duplex control, while **b** and **c** are retarded significantly. This would be the result if, for example, Y1 and T9 assumed a T shape, with the two arms formed by strand 1 resembling a duplex.

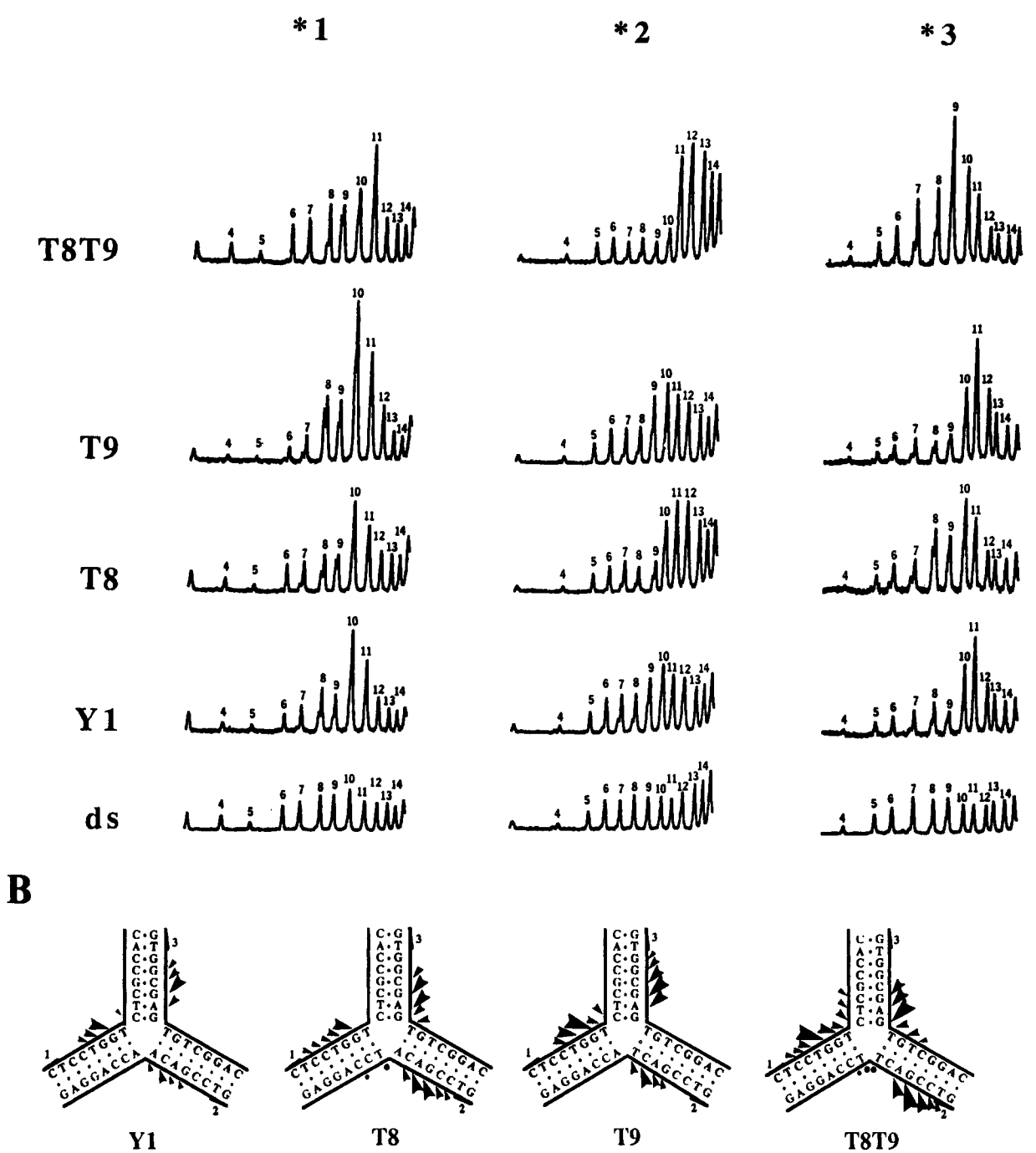

FIGURE 6: Cleavage of junctions by MPE·Fe(II). (A) Densitometric scans of the cleavage patterns of junctions due to MPE·Fe(II). Each panel of this figure corresponds to a given strand of junctions and contains five scans, corresponding to the junctions or duplexes of this study. The branch point lies between positions 8 and 9 on each strand. Note that strong enhancement of cleavage near branch sites is seen in all three-arm junctions relative to the full duplex and there is stronger enhancement of cleavage in mismatched T8, T9, and T8T9 relative to Y1. (B) Sites of preferential cleavage by MPE·Fe(II) in junctions are compared to those in the duplex. The same conventions apply to this figure as in Figure 5.

A more likely possibility, in view of the discussion below, is that it reflects the lifetime and configuration of transient structures forming in a dynamic equilibrium.

The two junctions T8 and T8T9 show a different mobility pattern. In T8, **a** is more severely retarded than **c**, while **b** moves more like an intact duplex. In a completely static model, this would imply that strand 2 forms a structure resembling a duplex, with sharper bending in the other arms. The most severe retardation occurs in T8T9, with T-T mismatches on two sides of the branch. In this case, **a** migrates extremely slowly, while **b**, and **c** maintain the mobilities seen in T8. Introducing one or more T-T mismatches thus has a variable effect on the relative mobility of these junctions, depending on the neighboring sequence.

Footprinting Experiments and Ligand Interactions. The conformation and geometry of branched DNAs have been investigated by chemical and enzymatic footprinting experiments (Galas & Schmitz, 1978). The strategy for branched complexes is to determine the pattern of reactivity of a probe by labeling each of the strands forming the complex, and comparing these with the fully duplex control formed by pairing each strand of the complex with its complementary strand (Lu et al., 1992). Here the patterns of the three junctions containing mismatches are compared with those of Y1 and the three-arm junction lacking mismatches, as well as the

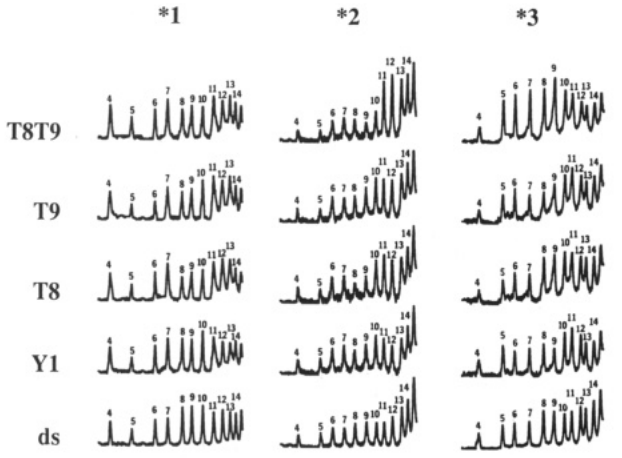

FIGURE 7: Densitometric scans of cleavage patterns by MPE·Fe(II) in the presence of tetrapyridylporphyrins (H_2TMpyP-4). The same conventions apply to this figure as to Figure 6A.

duplex controls. The differential patterns of Y1 relative to the three duplexes formed by each of its component strands have been reported (Guo et al., 1990); the control ds lane in each gel records the profile of reactivity of the intact duplex with the same sequence as the strands in Y1.

Figure 4 summarizes results of experiments in which the junctions in Figure 1 are exposed to a variety of reactive probes, including OsO_4, which is selective for T in the single-stranded state (Lilley & Palecek, 1984); diethyl pyrocarbonate, selective for purines in the single-stranded state (Herr, 1985); the single-strand-specific *N. crassa* endonuclease (Fraser, 1980); and the double-strand DNA-specific endonuclease DNase I [see Lu et al. (1989)]. Three of these reagents identify the state of base pairing in the junctions, while the third monitors the degree of protection from DNase I cleavage due to the presence of the branch (Lu et al., 1989). The OsO_4 reactivity pattern in Y1 reveals accessibility of the T's that flank the branch that are present in strands 1 and 3 (see Figure 1). The center panel shows the additional reactivity of the T's introduced in strand 2. The actual patterns indicate that a G adjacent to a reactive T can show enhanced activity; the bands at nonintegral positions correspond to incompletely hydrolyzed products. Thus, any T flanking the branch is reactive to OsO_4, whether or not it is involved in a mismatch. The DEPC experiment shows the enhanced reactivity of purines flanking the branch in Y1 as well as the three junctions with T-T mismatches. Note that distal sites become more reactive in Y1 and T9 than in T8 or T8T9, e.g., A11 and G12 in strand 2. The reactivity of G12 in strand 2 is higher in T8 and T9 than in either Y1 or T8T9, an observation that is not easy to reconcile with any static model for the structure in these junctions. The next panels show the reactivity of the junctions to a single-strand-specific nuclease, the *N. crassa* endonuclease, and to DNase I, which does not cleave at sites adjacent to a branch (Lu et al., 1989). Figure 5 summarizes the patterns in a graphic form, with sites of enhanced reactivity indicated by arrows, proportional in size to the activity seen in the gel assays, and sites of inhibition of activity indicated by circles, also proportional in size to the effect seen. Apart from obvious differences due to sequence *per se*, seen in the reactivity of T8, T9, and T8T9 to OsO_4 or DEPC, for example, it is evident that Y1 and T9 share a common set of patterns, while T8 and T8T9 resemble each other more than they do Y1 or T9. This similarity extends also to the mobility experiment in Figure 3B, implying that the substitution of T for A9 in strand 2 of Y1 has relatively little effect on the structure and geometry of Y1 relative to the substitution at A8.

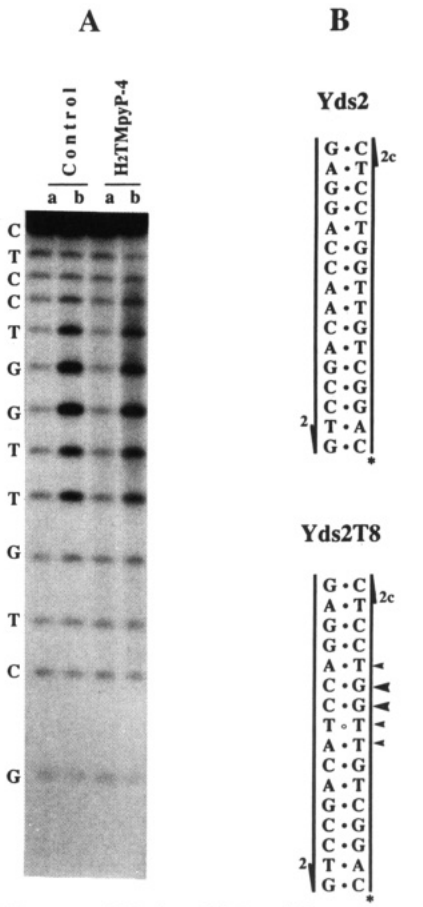

FIGURE 8: Cleavage of duplex Yds2 and its corresponding T-T mismatched duplex Yds2T8 by MPE·Fe(II) in the presence and absence of tetrapyridylporphyrin. (A) Autoradiograph of the gel. Duplexes 5′-labeled with ^{32}P in strand 2c only were cleaved by MPE·Fe(II) in the absence (control) and presence of tetrapyridylporphyrin (H_2TMpyP-4). Lanes a and b represent Yds2 and Yds2T8, respectively. Note that enhancements of cleavage are seen near the T-T mismatched site in Yds2T8 in both the presence and absence of tetrapyridylporphyrin. (B) Sequences of Yds2 and Yds2T8. Arrows indicate sites of preferential cleavage in Yds2T8 compared to those in the corresponding full duplex. The size of an arrow is a measure of the quantitative intensity of each responsive site.

The probe MPE·Fe(II) interacts with duplex DNA, cleaving the backbone at positions corresponding to ethidium intercalation sites (van Dyke & Dervan, 1983). Both three- and four-arm junctions show preferential interaction with this reagent at sites near the branch, detected as enhanced reactivity for this probe that is inhibited by ethidium itself (Guo et al., 1989). Figure 6A shows densitometer scans of gels in which the junctions with labeled strands indicated are exposed to MPE·Fe(II) cleavage. Figure 6B illustrates the results in graphic form. While each junction shows a pattern of enhanced reactivity that is strickly unique, the pattern for Y1 resembles that for T9, while T8 and T8T9 are less related. For example, note the strong enhancement at positions 10 and 11 in strand 3, with a greater effect at 11 than at 10, that occurs in Y1 and in T9, but not in T8 or T8T9. Thus, each junction retains a strong interaction site for ethidium near the branch.

In a previous study, it was reported that the branch in a four-arm junction interacts selectively also with a series of tetrapyridylporphyrins (Lu et al., 1990). The interaction is detected as a strong perturbation in the pattern of MPE·Fe(II) scission at sites in the vicinity of the branch when the

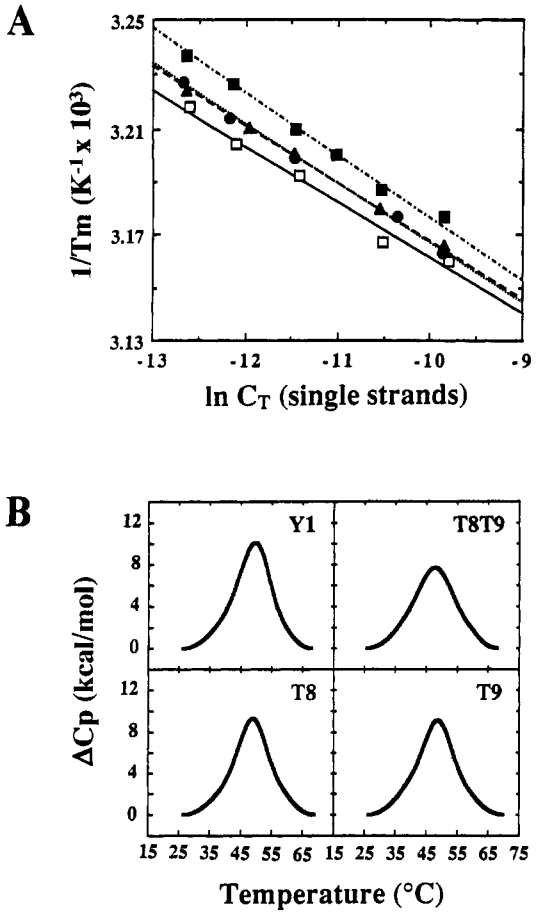

FIGURE 9: Thermodynamic studies of three-arm junctions. (A) Dependence of the transition temperature on strand concentration in 20 mM sodium cacodylate buffer containing 100 mM NaCl and 1 mM $MgCl_2$ (pH 7.0). The filled symbols represent junctions containing mismatches: (▲) T9; (●) T8; (■) T8T9. The open squares (□) represent Y1. (B) Differential heat absorption profiles for Y1 and the mismatched junctions in the above buffer.

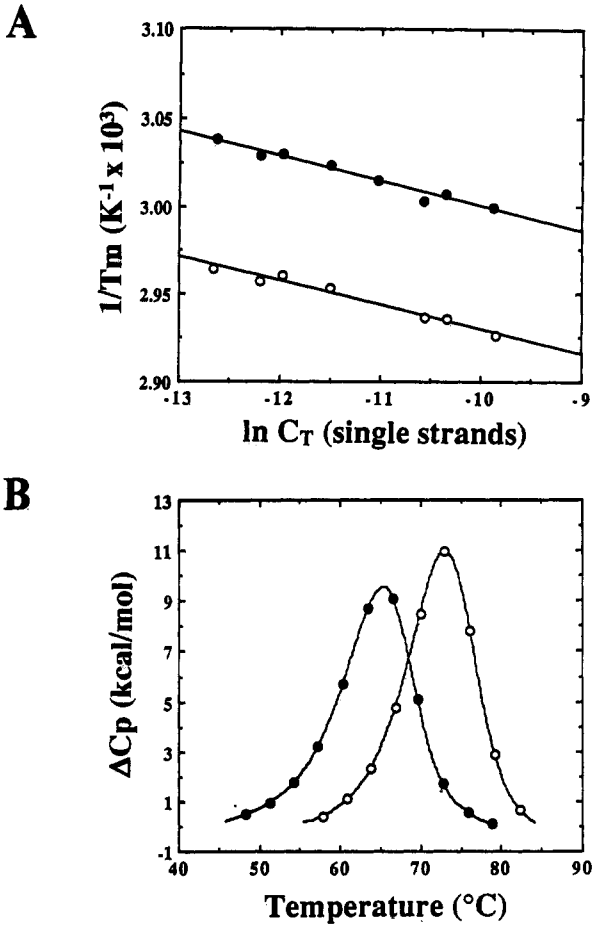

FIGURE 10: Thermodynamic studies of a fully duplex control (Yds2) and its corresponding T-T mismatched duplex (Yds2T8). (A) Dependence of the transition temperature on strand concentration. (B) Differential heat absorption profiles. The filled circles (●) represent Yds2T8 whereas the open circles (○) represent Yds2.

porphyrin is present. One might naively expect that mismatched bases will favor interaction of such bulky ligands at the branch, if steric factors alone are most important in binding. We tested this by adding an equimolar concentration of H_2-TMpyP-4 to MPE, and obtained the profiles shown in Figure 7. The general response in these junctions is loss of MPE reactivity near the branch. For example, Y1, T8, and T9 and T8T9 all show protection from scission at position 10 in strand 1 and positions 9–11 in strand 3. To determine whether a mismatch alone can account for this effect, we carried out the same experiment on the two duplexes Yds2 and Yds2T8, the sequences of which are shown in Figure 8B, with the result shown in Figure 8A. As has been reported previously, MPE·Fe(II) scission is enhanced at a T-T mismatched base pair in a duplex (Zhong et al., 1992). However, the enhancement observed turns out to be unaffected by the presence of the porphyrin (Figure 8), in contrast to the differential response seen in Y1 and the mismatched junctions. There is no indication of a differential response in T8T9 over T8 or T9, arguing that steric factors are not the exclusive ones.

Mismatches Have a Minor Destabilizing Influence on Three-Arm Junctions. To evaluate the stability of the junctions, we monitored the thermal unfolding of junctions relative to 16mer duplexes with and without a mismatch in two ways. First, the concentration dependence of the unfolding of Y1 was measured by UV spectroscopy as described under Materials and Methods, and compared with that of the mismatched species (Figure 9A) and the duplex controls (Figure 10A) to estimate the van't Hoff enthalpies of formation of each complex (Marky & Breslauer, 1987). As discussed previously, these enthalpies are model-dependent because they assume two-state transition behavior in each case. Model-independent enthalpies were derived by differential calorimetric measurements, as shown in Figures 9B and 10B. The results are summarized in Table I, which compares the van't Hoff and calorimetric parameters for forming each complex from an equimolar mixture of strands at 20 °C. The concentration-derived enthalpies are larger than the calorimetric values, as has been observed in many duplexes and branched molecules (Zhong et al., 1992). We attribute this effect to the contribution of intermediate states to the UV transition. The differential heats tabulated as $\Delta\Delta H°$ show excellent agreement between the calorimetric and van't Hoff values. There is a clear loss in enthalpy on introducing a mismatch at the branch, and this is a additive in the T8T9 complex. The loss in enthalpy is almost completely compensated by a decrease in the unfavorable entropy of forming the complexes containing mismatches. The resultant effect on the free energy is small, and there is indeed no discernible difference in stability between T8, T9, or T8T9 at 20 °C (Table I). Each of these is roughly 2 kcal/mol less stable than Y1, a small difference that is barely within the error limits of measurement. Nevertheless, the thermodynamics of forming a complex with a mismatch are clearly distinctive in terms of the lower enthalpy and entropy changes involved. For comparison, the corresponding thermodynamic

Table I: Thermodynamic Parameters for Junction Formation at 20 °C[a]

	calorimetry					UV spectroscopy	
junction	T_m (°C)	$\Delta H°_{cal}$ (kcal/mol)	$\Delta\Delta H°_{cal}$ (kcal/mol)	$\Delta G°$ (kcal/mol)	$T\Delta S°$ (kcal/mol)	$\Delta H°_{vH}$ (kcal/mol)	$\Delta\Delta H°_{vH}$ (kcal/mol)
Y1	50	−156		−15	−141	−189	
T8	49	−145	11	−13	−132	−176	13
T9	49	−148	8	−13	−135	−181	8
T8T9	48	−136	20	−13	−123	−169	20
Yds2	73	−121		−18	−103	−145	
Yds2T8	65	−115	6	−15	−100	−138	7

[a] All measurements were done in 20 mM sodium cacodylate buffer containing 100 mM NaCl and 1 mM $MgCl_2$ at pH 7.0. The calorimetric T_m's correspond to a total strand concentration of 283 μM (three-arm junctions) or 214 μM (duplexes). The $\Delta H°_{cal}$ values are averages of five determinations and are within ±3%; the $T\Delta S°$ values are within 5% experimental error. Spectroscopic $\Delta H°_{vH}$ values were determined from plots of $1/T_m$ vs ln C_T; these van't Hoff enthalpies are estimated to be within ±10% experimental error. The $\Delta\Delta H°_{cal}$ and $\Delta\Delta H°_{vH}$ values are relative to the corresponding enthalpies for Y1 or Yds2.

parameters for forming the duplex Yds2 and the mismatched duplex Yds2T8 are also provided in the table. The duplex is more stable than the mismatched duplex, by about 3 kcal/mol. The loss in enthalpy accompanying a mismatch in a duplex is smaller than in formation of a mismatch flanking the branch in these junctions.

DISCUSSION

If it is admitted that the properties of three-arm branches in DNA warrant investigation, the fact that their conformational properties differ in essential ways from those of duplexes or four-arm branched structures is not without interest. An analysis of structures containing short branches has suggested that the process of forming a three-arm branch is not static or comparable to what happens in a four-arm branch. From a series of mobility experiments, Duckett and Lilley (1990) decided that three-arm junctions are essentially fully open, lacking base pairs at the branch. More extensive experiments, including those reported here, suggest that the actual case is not so simple. Indications that there are interactions among bases at the branch come from the mobility experiments in Figure 3, the patterns of reactivity to single-strand probes in Figure 5, and the interaction of these structures with methidium, seen in Figure 6. Characteristics of the structure in three-arm junctions thus include (i) asymmetry in disposition of the arms, (ii) at least partial unpairing of bases at the branch, (iii) flexibility in angle at the branch, and (iv) asymmetry in reactivity to MPE·Fe(II).

One proposal that explains the above properties comes from experiments on very short branches (Zhong & Kallenbach, 1993). Rather than simply pairing to create a new double-helical arm, the bases that emanate from the "parent" interact with base pairs at the branch site in the duplex. Opening at a three-arm branch can then be understood to be transient, since there is a distribution of states present at any time. The stability of the base pairs flanking the branch, as well as their neighbors, is involved in the equilibrium. In terms of this model, a mismatch introduces a new perturbation to the system. Rather than simply relaxing conformational strain, as we originally thought it might, or limiting its effect to weakening a particular arm, as in a static, rigid model, the mismatch can reduce the contribution of some states, and enhance others. This allows us to explain the observation that the configuration of T9 resembles that of Y1, while T8 looks more like T8T9 in a different way. The T9 mismatch in arm II reduces the ability of bases in that arm to compete with the favored stacked duplex anchored by arms I and III; in both cases, complex **a** is seen to have the highest mobility (Figure 3), or the least deformation from linearity. Since the T8 mismatch reduces the stacking between arms I and II, the preferred "duplex" is formed from arms I and II, so that **b** represents the least deformed species. The fact that **b** migrates fastest in T8T9 implies that the mismatch at T8 exerts a stronger effect; the presence of T9 does not change the relative mobility of species **b** or **c**. However, since species **a** migrates more slowly in T8T9, there is a rearrangement in geometry relative to T8 or T9, interpreted now as a change in dynamics of the arms.

Compared to the effect of a T-T mismatch at the branch in a four-arm model junction, a T-T mismatch has a smaller destabilizing influence on a three-arm junction (Table I). This results from a reduction in both $\Delta H°$ and $\Delta S°$ for formation of the junction. The loss in enthalpy of forming a junction with a mismatch seems understandable, since an A-T pair is disrupted, even if it is only partially paired in Y1. The enthalpy difference for formation of T8T9 compared to Y1 is very nearly the sum of the individual enthalpy decreases for T8 and T9. In each case, the difference is about half that observed for T-T mismatches in a four-arm junction, but more than for this mismatch in a duplex (Zhong et al., 1992). The decrease in entropy which compensates for the enthalpy loss is less easily understood. One source of such an effect is differences in the hydration of the branch in the junctions studied. A second is the change in the contributing conformations due to the mismatch(es). If the three-arm structure reflects a mix of contributions from several substates in which different flanking pairs are disrupted, the consequences of introducing a mismatch are not easily predictable. In particular, loss of a pair at the branch can enhance certain conformers that depend on breaking that pair to produce an intermediate for insertion into another duplex, while disfavoring others. As noted above, the similarity in both conformation and reactivity patterns between Y1 and T9 argues that A9 in strand 2 of Y1 has a relatively minor role in interaction with the duplex formed from arms I and II in Figure 1. Conversely, A8 is implicated as more important because its substitution by T in T8 leads to a gross change in both geometry and reactivity. The small difference in the free energy of stabilization detected between T8T9 and either single substitution is consistent with the hypothesis that a dynamic ensemble of states is involved; in a static model, T8T9 should be destabilized relative to T8 and T9, in the same way that its enthalpy decreases as the sum of the individual differences (Table I).

The thermodynamic profiles in Figure 9B show how branches can influence the thermal transitions in a DNA duplex. While there is little to distinguish the profiles of Y1 from those of T8 or T9, the double mutant T8T9 has a broader transition profile than any of the other species. Since these molecules differ at specific sites only, the increase in width seems to be due to an increase in the number of intermediate conformations accessible to T8T9. By increasing the popu-

lation of intermediates, single-stranded hairpins can influence the transition profile in a long duplex that contains palindromes.

All the junctions of this study are able to bind large ligands such as porphyrins more tightly at the branch than duplexes or duplexes containing mismatches. The fact that duplex DNA can bind tetrapyridylporphyrins intercalatively seems surprising in the first place, given the size of the ring system. Nevertheless, the evidence that the ring system intercalates seems persuasive (Fiel, 1989; Banville et al., 1986). The ability of the junctions containing mismatches to accommodate tetrapyridylporphyrins about as easily as Y1 itself supports our suggestion that the conformation at the branch is not static. As described by Fiel (1989) and others, the rate-limiting step in insertion of a porphyrin ring is likely to be opening of the duplex to allow passage of the ring system together with its substituent groups. The motion involved would seem to entail unpairing of at least one and possibly more base pairs in the duplex. Why then does the presence of a single T-T mismatch in a duplex not alter the pattern of MPE scission of the duplex itself in the presence of porphyrin (Figure 8)? Steric factors cannot be the sole consideration in a process such as intercalative binding of a porphyrin. The relatively open state at the branch in three-arm junctions might play a role, but the response of these three-arm junctions is quite different from that of four-arm junctions, where strong enhancement in MPE scission is observed (Lu et al., 1990). The ability of three-arm junctions to bind porphyrin more tightly than duplex DNA is likely to reflect several factors besides the size of the pocket itself, and these remain to be investigated.

ACKNOWLEDGMENT

We thank Dr. Luis Marky for helpful discussions and for assistance with the calorimetric measurements.

REFERENCES

Aboul-Ela, F., Koh, D., & Tinoco, I., Jr. (1985) *Nucleic Acids Res. 13*, 4811–4824.

Banville, D. L., Marzilli, L. G., Strickland, J. A., & Wilson, W. D. (1986) *Biopolymers 25*, 1837–1858.

Breslauer, K. J., Frank, R., Blocker, H., & Marky, L. A. (1986) *Proc. Natl. Acad. Sci. U.S.A. 83*, 3746–3650.

Broker, T. R., & Doermann, A. H. (1975) *Annu. Rev. Genet. 9*, 213–244.

Cantor, C., Warshaw, M. W., & Shapiro, H. (1970) *Biopolymers 9*, 1059–1077.

Caruthers, M. H. (1982) in *Chemical and Enzymatic Synthesis of Gene Fragments* (Gassen, H. G., & Lang, A., Eds.) pp 71–79, Verlag Chemie, Weinheim.

Cooper, J. P., & Hagerman, P. J. (1987) *J. Mol. Biol. 198*, 711–719.

Copper, J. P., & Hagerman, P. J. (1989) *Proc. Natl. Acad. Sci. U.S.A. 86*, 7336–7340.

Doktycz, M. J., Goldstein, R. F., Paner, T. M., Gallo, F. J., & Benight, A. S. (1992) *Biopolymers 32*, 849–964.

Draper, D. E. (1992) *Acc. Chem. Res. 25*, 201–207.

Duckett, D. R., & Lilley, D. M. J. (1990) *EMBO J. 9*, 1659–1664.

Duckett, D. R., & Lilley, D. M. J. (1991) *J. Mol. Biol. 221*, 149–161.

Duckett, D. R., Murchie, A. I. H. Diekmann, S., von Kitzing, E., Kemper, B., & Lilley, D. M. J. (1998) *Cell 55*, 79–89.

Fiel, R. J. (1989) *J. Biomol. Struct. Dyn. 6*, 1259–1275.

Fraser, M. J. (1980) *Methods Enzymol. 65*, 255–263.

Galas, D. J. & Schmitz, A. (1978) *Nucleic Acids Res. 3*, 3157–3170.

Gluick, T. C., & Draper, D. E. (1992) *Current Opin. Struct. Biol. 2*, 338–344.

Goldstein, R. F., & Benight, A. S. (1992) *Biopolymers 32*, 1679–1693.

Gotoh, O. & Tagashira, Y. (1981) *Biopolymers 20*, 1033, 1042.

Guo, Q., Seeman, N. C., & Kallenbach, N. R. (1989) *Biochemistry 28*, 2355–2359.

Guo, Q., Lu, M., Churchill, M. E. A., Tullius, T. D., & Kallenbach, N. R. (1990) *Biochemistry 29*, 10927–10934.

Herr, W. (1985) *Proc. Natl. Acad. Sci. U.S.A. 82*, 8009–8013.

Jensch, F., & Kemper, B. (1986) *EMBO J. 5*, 181–189.

Koo, H.-S., Wu, H.-M., & Crothers, D. M. (1986) *Nature 320*, 501–506.

Leontis, N. B., Kwok, W., & Newman, J. S. (1991) *Nucleic Acids Res. 19*, 759–766.

Lilley, D. M. J., & Palecek, E. (1984) *EMBO J. 3*, 1187–1192.

Lu, M., Guo, Q., & Kallenbach, N. R. (1989) *J. Biol. Chem. 264*, 20851–20854.

Lu, M., Guo, Q., Pasternack, R. F., Wink, D. J., Seeman, N. C., & Kallenbach, N. R. (1990) *Biochemistry 29*, 1614–1624.

Lu, M., Guo, Q., & Kallenbach, N. R. (1991) *Biochemistry 30*, 5815–5820.

Lu, M., Guo, Q., & Kallenbach, N. R. (1992) *Crit. Rev. Biochem. Mol. Biol. 27*, 157–190.

Ma, R.-I., Kallenbach, N. R., Sheardy, R. D., Petrillo, M. L., & Seeman, N. C. (1986) *Nucleic Acids Res. 14*, 9745–9753.

Marky, L. A., & Breslauer, K. J. (1987) *Biopolymers 26*, 1601–1620.

Marky, L. A., Kallenbach, N. R., McDonough, K. A., Seeman, N. C., & Breslauer, K. J. (1987) *Biopolymers 26*, 1621–1634.

Maxam, A. M., & Gilbert, W. (1980) *Methods Enzymol. 65*, 499–560.

Minagawa, T., Murakami, A., Ryo, Y., & Yamagishi, H. (1983) *Virology 126*, 183–193.

Mizuuchi, K., Mizuuchi, M., & Gellert, M. (1982) *J. Mol. Biol. 156*, 229–243.

Saiki, R. K., Gelfand, D. H., Stoffel, S., Scharf, S. J., Higuchi, R., Horn, G. T., Mullis, K. B., & Erlich, H. A. (1988) *Science 239*, 487–491.

van Dyke, M. W., & Dervan, P. B. (1983) *Nucleic Acids Res. 11*, 5555–5567.

Woodson, S. A., & Crothers, D. M. (1989) *Biopolymers 28*, 1149–1177.

Zhong, M., & Kallenbach, N. R. (1993) *J. Mol. Biol. 230*, 766–778.

Zhong, M., Rashes, M. S., Marky, L. A., & Kallenbach, N. R. (1992) *Biochemistry 31*, 8064–8071.